PRAMANA
— journal of
physics

Vol. 61, No. 6
December 2003
pp. 1129–1144

Magnetic relaxation in a three-dimensional ferromagnet with weak quenched random-exchange disorder

S N KAUL* and ANITA SEMWAL
School of Physics, University of Hyderabad, Central University P.O., Hyderabad 500 046, India
*Present address: Departamento CITIMAC, Facultad de Ciencias, Universidad de Cantabria, 39005 Santander, Spain
Email: kaulsn@unican.es; kaulsp@uohyd.ernet.in

MS received 24 March 2003; revised 3 July 2003; accepted 31 July 2003

Abstract. Isothermal remanent magnetization decay, $M_r(t)$, and 'in-field' growth of zero-field-cooled magnetization, $M_{ZFC}(t)$, with time have been measured over four decades in time at temperatures ranging from $0.25T_c$ to $1.25T_c$ (where T_c is the Curie temperature, determined previously for the same sample from static critical phenomena measurements) for a nearly ordered intermetallic compound Ni_3Al, which is an experimental realization of a three-dimensional $(d = 3)$ ferromagnet with weak quenched random-exchange disorder. None of the functional forms of $M_r(t)$ predicted by the existing phenomenological models of relaxation dynamics in spin systems with quenched randomness, but only the expressions $M_r(t) = M_0[M_1 \exp(-t/\tau_1) + (t/\tau_2)^{-\alpha}]$ and $M_{ZFC}(t) = M_0'[1 - \{M_1' \exp(-t/\tau_1') + (t/\tau_2')^{-\alpha'}\}]$ closely reproduce such data in the present case. The most striking features of magnetic relaxation in the system in question are as follows: Aging effects are absent in both $M_r(t)$ and $M_{ZFC}(t)$ at all temperatures in the temperature range covered in the present experiments. A cross-over in equilibrium dynamics from the one, characteristic of a pure $d = 3$ ferromagnet with complete atomic ordering and prevalent at temperatures away from T_c, to that, typical of a $d = 3$ random-exchange ferromagnet, occurs as $T \to T_c$. The relaxation times $\tau_1(T)(\tau_1'(T))$ and $\tau_2(T)(\tau_2'(T))$ exhibit logarithmic divergence at critical temperatures $T_c^{\tau_1}(T_c^{\tau_1'}(H))$ and $T_c^{\tau_2}(T_c^{\tau_2'}(H))$; $T_c^{\tau_1'}$ and $T_c^{\tau_2'}$ both increase with the external magnetic field strength, H, such that at any given field value, $T_c^{\tau_1'} = T_c^{\tau_2'}$. The exponent characterizing the logarithmic divergence in $\tau_1'(T)$ and $\tau_2'(T)$ possesses a field-independent value of $\simeq 16$ for both relaxation times. Of all the available theoretical models, the droplet fluctuation model alone provides a qualitative explanation for some aspects of the present magnetic relaxation data.

Keywords. Magnetic relaxation; spin dynamics; random-exchange ferromagnet; remanent magnetization decay; time evolution of zero-field-cooled magnetization.

PACS Nos 75.40.Gb; 75.60.Lr; 75.50.Lk; 75.50.Cc

1. Introduction

Extensive experimental investigations [1–10] of magnetic relaxation in spin glasses have clearly brought out several important aspects of the inherently slow spin dynamics and aging phenomenon (i.e., the dependence of the relaxation response, measured after a wait

time, t_w, on t_w) in such materials. The theoretical input required for understanding the non-equilibrium behavior of spin glasses has been provided by the droplet models [11–13]. In these theoretical approaches, aging results from the growth of spin-glass domains with time; the size of the domains determines the maximum length scale over which the system possesses equilibrium properties. Another crucial concept introduced by these theories, and vindicated by experiments [5,6,10] and Monte Carlo simulations [14], is the overlap length, which determines the maximum length scale over which the equilibrium spin-glass domains in the presence of an external perturbation (such as temperature ΔT or magnetic field ΔH or exchange bond ΔJ) are practically indistinguishable from those in the unperturbed state. Despite a great deal of success enjoyed by the droplet models, certain aspects of the aging phenomenon in spin glasses are better described [7] by a model that invokes a hierarchical organization of metastable states in phase space. While a common consensus about the spin dynamics in spin glasses is slowly emerging, the understanding of relaxation phenomena in random-exchange ferromagnets is far from being complete, as elucidated below.

In random-exchange ferromagnets (which include both quenched random site-diluted and bond-diluted ferromagnets) that exhibit re-entrant behavior at temperatures well below the Curie point, T_c, a thermally-induced cross-over has been observed [15–17] between two distinct dynamics regimes: regime I, marked by a power-law temporal decay of the thermoremanent magnetization (TRM) with negligible aging effects for temperatures close to T_c, characterizing a high-temperature ferromagnetic phase, and regime II, signalled, at low temperatures, by a stretched exponential TRM decay with time and non-equilibrium age-dependent dynamics (i.e., properties typical of spin glasses), characterizing the re-entrant phase. While the power law TRM decay and the absence of aging effects are consistent with the prediction of the droplet fluctuation model [18] for an Ising ferromagnet with quenched random-exchange disorder, the stretched exponential TRM decay and the aging phenomenon find a straightforward explanation within the framework of the droplet scaling or domain or hierarchical models [7,11–13]. Neither the former model nor the latter theoretical treatments offer any explanation for the cross-over between a high-temperature regime (ferromagnetic phase) of equilibrium dynamics to a low-temperature regime (re-entrant phase) of non-equilibrium dynamics. On the other hand, the percolation model [19] for relaxation in random systems (that deals with the relaxation of isotropic, low-energy dispersive excitations (magnons) within domains distributed in size with a probability dictated by the percolation theories, and assumes that each domain relaxes independently with a relaxation rate which varies exponentially with inverse domain size and thereby takes into account the finite-size quantization of elementary excitations) reproduces [15,16] the power law (stretched exponential) TRM decay when the dynamics is dominated by the domains aligned along (antiparallel to) the magnetic field direction, but fails to account for the aging effects in the re-entrant phase. Recognizing the fact that the studies of magnetic relaxation have so far been confined to the strongly disordered random-exchange (e.g., spin glasses or re-entrant ferromagnets) spin systems only, an extensive magnetic relaxation study has been undertaken on a ferromagnet with weak quenched random-exchange disorder. This study addresses itself to not only the thermoremanent magnetization decay but also the time-evolution of zero-field-cooled magnetization from the time $(t = 0)$ at which a magnetic field of given strength is suddenly switched on. Such experiments are shown to reveal a number of new and novel aspects of magnetic relaxation in the ferromagnetic system under consideration.

2. Experimental details

Polycrystalline sample of the $Ni_{75}Al_{25}$ (actual composition: $Ni_{75.08}Al_{24.92}$) alloy was prepared in the form of a rod of 10 mm diameter and 100 mm length from ultra-high-purity (99.999%) nickel and aluminium by radio frequency induction technique. A sphere of 3 mm diameter and a disc of 10 mm diameter and 5 mm thickness were spark-cut from the rod, annealed at 520°C for 16 days in quartz tube evacuated to a pressure of 10^{-7} Torr and subsequently water-quenched. An elaborate analysis of the X-ray diffraction patterns taken on the disc sample yielded the value for the long-range atomic order parameter as $S = 0.95 \pm 0.02$. Details about the preparation and characterization of the samples in question are given elsewhere [20]. In a completely ordered Ni_3Al intermetallic compound, Ni and Al atoms respectively occupy face centers (A sites) and corners (B sites) of the face centered cubic unit cell. Thus, A and B sites form the Ni and Al sublattices. In a partially ordered $Ni_{75}Al_{25}$ alloy, if the number of right atoms (Ni atoms on A sites, Al atoms on B sites) and wrong atoms (Ni atoms on B sites, Al atoms on A sites) on a given sublattice are denoted by r and w, the total number of atoms on the A or B sites is given by $n = r + w$. The long-range order parameter, defined as $S = (r - w)/n = (2r/n) - 1$, equals unity for the completely ordered case when $r = n$. In view of this standard definition, the observed value of S indicates that in the present sample, 97.5 ± 1.0 (2.5 ± 1.0)% of A or B sites are occupied by Ni (Al) or Al (Ni) atoms. The wrong atoms generate site disorder and in the sample under consideration they give rise to quenched random-exchange disorder since Ni atoms are magnetic while Al atoms are non-magnetic. Now that the percentage of the wrong atoms is very small, random-exchange disorder is weak. The following types of magnetic relaxation measurements have been performed on the annealed (nearly ordered) sample of spherical shape, using the PAR 4500 vibrating sample magnetometer system.

(i) *Isothermal remanent magnetization decay*: After cooling the sample to a desired temperature T_m from temperatures as high as $2T_c$ in zero-field, a magnetic field of fixed strength in the range 15 Oe $\leq H \leq$ 15 kOe is applied after a wait time t_w and then dropped to zero within a time period that ranges from 15 s to 2 min depending upon the field strength. The decay of remanent magnetization with time at $T = T_m$ from this time (when the externally applied field was brought down to zero) $(t = 0)$ onwards is recorded. This mode of measurement is henceforth referred to as the 'unconventional' method. The conventional method of measuring isothermal remanent magnetization decay has also been used. In this method, sample is cooled in a fixed field in the range 15 Oe $\leq H \leq$ 15 kOe from $T \cong 2T_c$ to T_m and after a wait time t_w, the field is brought down to zero. The remanent magnetization is measured as a function of time starting from the time $t = 0$ when the field is zero.

(ii) *Time evolution of magnetization in field*: Sample is cooled in zero-field from a temperature much higher than T_c $(T \cong 2T_c)$ to the measuring temperature (T_m), and after a wait time t_w, a static magnetic field is applied. The evolution of zero-field-cooled magnetization (M_{ZFC}) with time is recorded from the time $(t = 0)$ the field has reached the desired value. With a view to ascertaining whether the aging effects are important, t_w is varied from 0 to 2 h.

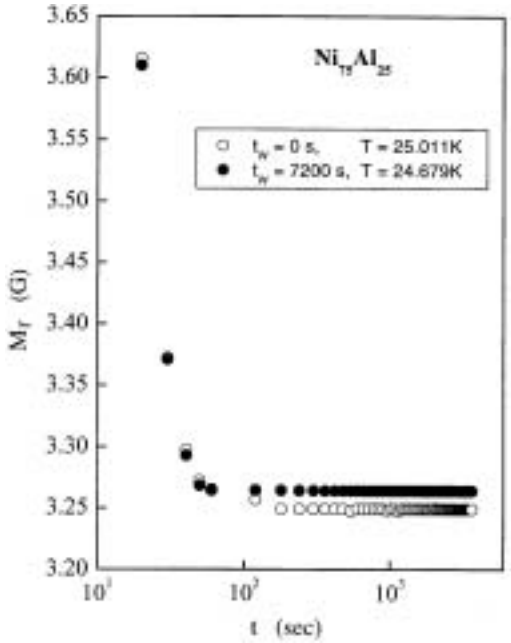

Figure 1. Representative plots of $M_r(t)$ at $T \simeq 25$ K and widely different wait time, t_w, values. A total absence of aging effects is evidenced by the fact that the temperature difference of 0.332 K completely accounts for the discrepancy between the $M_r(t)$ values at $t > 100$ s.

3. Results and discussions

Both the above-mentioned methods of measuring the decay of isothermal remanent magnetization with time, $M_r(t)$, yield exactly the same results and no aging effects could be detected at any temperature. As an illustration of no aging effects in the time decay of isothermal remanent magnetization, figure 1 displays the $M_r(t)$ curves for the wait times $t_w = 0$ s and $t_w = 7200$ s taken at 25 K. Moreover, the magnetic field history of the sample affects only the magnitude of M_r but not its functional dependence on t. Another important point to note is that due to the weak M_r signal when the sample is exposed to fields $\leq$100 Oe prior to $M_r(t)$ measurements particularly at temperatures close to T_c, poor signal-to-noise ratio severely limits the time window over which $M_r(t)$ can be accurately measured. Hence, figure 2 depicts the representative $M_r(t)$ data taken at different but fixed temperatures over three decades of time in seconds, i.e., in the time interval 10^1 s $\leq t \leq 10^4$ s, when $t_w = 0$ and a field $H = 15$ kOe was applied before measuring $M_r(t)$ using the so called unconventional method. First of all, an attempt was made to fit the $M_r(t)$ data to the expressions used in the literature [1–19] (i.e., stretched exponential, power law, power law-stretched exponential product) to describe isothermal remanent magnetization decay in spin glasses and re-entrant ferromagnets. Strong departures of the present $M_r(t)$ data from the best fits based on these expressions permitted us to rule out all these possibilities. This inference is consistent with the observation that the sample in question does not exhibit any of the characteristic attributes of either spin glasses or re-entrant ferromagnets.

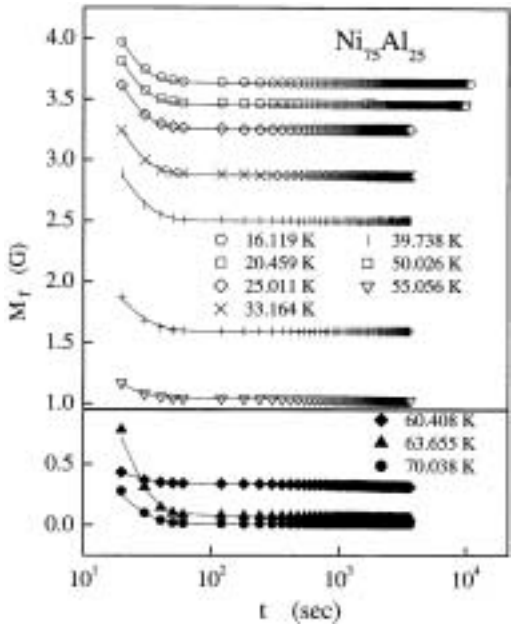

Figure 2. Time dependence of remanent magnetization at different temperatures $(t_w = 0)$.

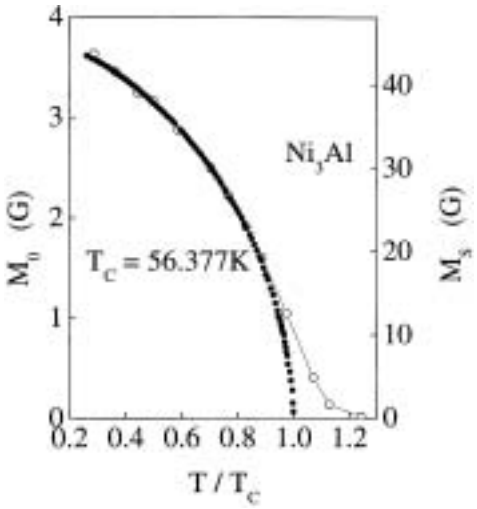

Figure 3. Remanent magnetization at $t_w = 0$ s (open circles), as a function of reduced temperature T/T_c. Solid circles represent the spontaneous magnetization data taken from [20].

Having exhausted all possible combinations of the expressions for $M_r(t)$ reported in the literature, we finally arrive at the following combination:

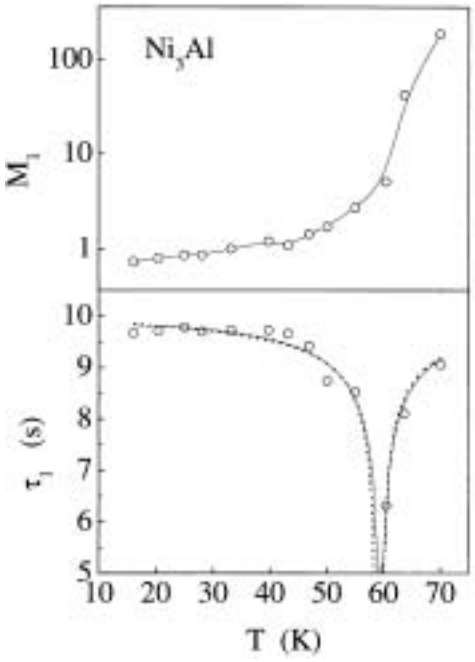

Figure 4. Prefactor, M_1, and relaxation time, τ_1, as functions of temperature. The solid (dotted) curve in the lower panel represents the logarithmic fit (power law fit).

$$M_{\rm r}(t) = M_0 \left[M_1 \exp(-t/\tau_1) + (t/\tau_2)^{-\alpha} \right] , \tag{1}$$

which reproduces quite well the observed time dependence of remanent magnetization at all the measuring temperatures, as is evident from figure 2 where the best least-squares fits, based on eq. (1), are depicted as continuous curves through the $M_{\rm r}(t)$ data (symbols). Note that these fits deviate from the $M_{\rm r}(t)$ data taken at $t < 20$ s; such deviations have been attributed to the uncertainty in fixing the zero of time accurately and to the decay of stray fields. Hence the $M_{\rm r}(t)$ data taken at $t < 20$ s have been left out of the analysis. The values of the parameters M_0, M_1, τ_1, τ_2 and α at different temperatures corresponding to the fits based on eq. (1) are displayed in figures 3–5. The main salient features that the data shown in these figures present are the following: (i) For temperatures $T \leq 0.9T_{\rm c}$ (Curie temperature $T_{\rm c} = 56.377$ K, as determined [20] from the detailed analysis of the spontaneous magnetization, $M_{\rm s}(T)$, data in the critical region), M_0 scales with $M_{\rm s}$ while the remaining parameters possess nearly temperature-independent magnitudes of $M_1 \cong 1$, $\tau_1 \cong 9.8$ s, $\tau_2 \cong 10^{-4}$ s and $\alpha \cong 10^{-6}$. (ii) For $T > 0.9T_{\rm c}$, M_0 decays to zero at $T \cong 1.2T_{\rm c}$, M_1 and α increase by several orders of magnitude and τ_1 and τ_2 exhibit a singular behavior. It immediately follows from the observations (i) and (ii) that (a) the contribution to $M_{\rm r}(t)$ due to the first term in eq. (1) overshadows the one arising from the second term for $T \leq 0.9T_{\rm c}$, (b) the latter contribution (the power law contribution) rapidly picks up in magnitude and dominates over the first for temperatures in the immediate vicinity of $T_{\rm c}$, and (c) the exponential term again essentially governs the time dependence of $M_{\rm r}$ for $T > T_{\rm c}$. The deductions (a), (b) and (c) are made all the more obvious by the data displayed in figures 6, 7 and 8, respectively. These figures show the percentage deviation of the

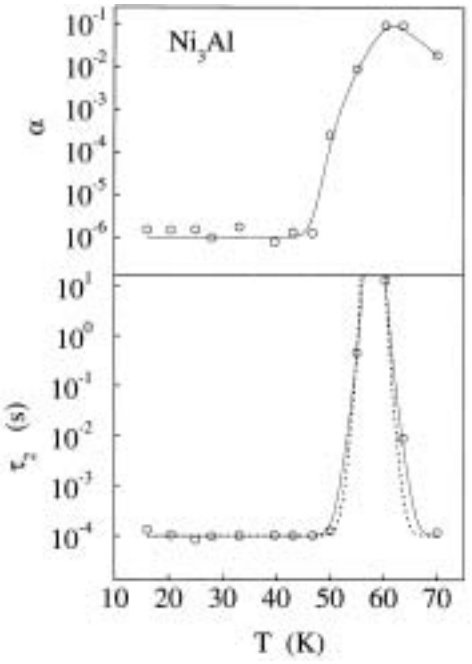

Figure 5. Exponent, α, and relaxation time, τ_2, as functions of temperature. The solid (dotted) curve in the lower panel represents the logarithmic fit (power law fit).

experimental $M_r(t)$ data taken at temperatures 28.053 K ($T \ll T_c$), 60.408 K ($T \approx T_c$) and 70.038 K ($T \gg T_c$) from the best least-squares fits to the $M_r(t)$ data based on either the exponential term alone or the power law term alone or the combination of the two, as in eq. (1). Even a cursory glance at these figures suffices to reveal that the deviations are the least and statistically distributed around zero for the exponential fit at 28.053 K ($T \ll T_c$) and 70.038 K ($T \gg T_c$), and for the fit based on eq. (1) (or more so, for the power law fit for $t > 500$ s) at 60.408 K ($T \approx T_c$). The deviation plots shown in figures 6–8 thus demonstrate that the power law decay (the second term in eq. (1)) and the exponential decay (the first term in eq. (1)) essentially determine the temporal behavior of remanent magnetization within and outside the critical region, respectively. However, this inference does not imply that the exponential (power law) decay is absent within (outside) the critical region. That this is indeed the case, is evident from figures 7 and 8 where the inclusion of the exponential term, besides the power law term, yields considerably lower deviations for $t < 500$ s at $T = 60.408$ K whereas the exponential term makes a significant contribution only for $t \leq 60$ s at $T = 70.038$ K; for $t > 60$ s at the same temperature, it is difficult to distinguish between the pure power law and pure exponential fits.

An attempt has been made to analyse the singular behavior of the relaxation times τ_1 and τ_2 in terms of the following expressions:

$$\tau(T) = A[\ln|(T - T_c^{\tau})|/T_c^{\tau}]^B + C \tag{2}$$

and

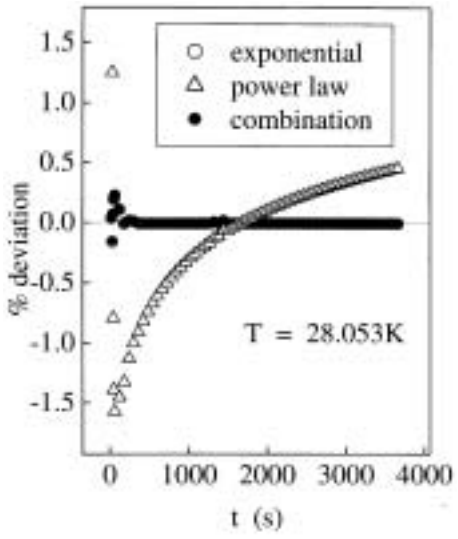

Figure 6. Percentage deviation of the experimental $M_r(t)$ data taken at 28.053 K $(T < T_c)$ from the fits based on pure exponential (first term in eq. (1) alone), pure power law (second term in eq. (1) alone) and a combination of the two (eq. (1)).

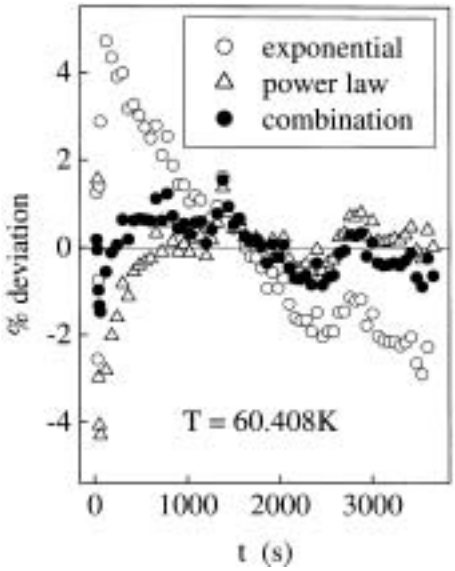

Figure 7. Percentage deviation of the experimental $M_r(t)$ data taken at 60.408 K $(T \approx T_c)$ from the fits based on pure exponential (first term in eq. (1) alone), pure power law (second term in eq. (1) alone) and a combination of the two (eq. (1)).

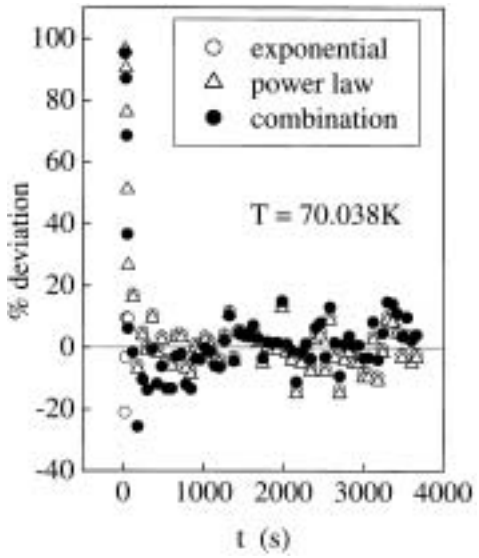

Figure 8. Percentage deviation of the experimental $M_r(t)$ data taken at 70.038 K $(T > T_c)$ from the fits based on pure exponential (first term in eq. (1) alone), pure power law (second term in eq. (1) alone) and a combination of the two (eq. (1)).

Table 1. Optimum fit parameters appearing in eqs (2) and (3). The numbers in the parentheses denote the uncertainty in the least significant figure. $\chi^2_r = \{\sum_i[(y_i(\text{obs}) - y_i(\text{cal}))^2/(y_i(\text{obs}))^2]\}/(N - N_p)$. N is the total number of data points in the temperature range of the fit and N_p is the number of free fitting parameters.

	A (s)	T_c^τ (K)	B	C (s)	χ^2_r (10^{-4})	a (s)	T_c^τ (K)	b	c (s)	χ^2_r (10^{-2})
τ_1										
Logarithmic divergence, eq. (2)	−0.25(1)	59.5(1)	1.9(1)	9.9(1)	5.01	−0.25(1)	59.5(1)	1.9(1)	9.9(1)	5.01
Power law divergence, eq. (3)	−0.48(1)	59.1(2)	−0.55(5)	10.4(1)	6.15	−0.48(1)	59.1(2)	−0.55(5)	10.4(1)	6.15
τ_2										
Logarithmic divergence, eq. (2)	1.4(1) $\times 10^{-11}$	58.4(1)	23(1)	1.0(1)	1.88	1.4(1) $\times 10^{-11}$	58.4(1)	23(1)	1.0(1)	1.88
Power law divergence, eq. (3)	1.5(1) $\times 10^{-15}$	58.1(1)	−11(1)	1.0(1)	7.68	1.5(1) $\times 10^{-15}$	58.1(1)	−11(1)	1.0(1)	7.68

$$\tau(T) = a\,[(T - T_c^\tau)/T_c^\tau]^b + c, \tag{3}$$

where τ stands for τ_1 or τ_2. The best least-squares fits based on eqs (2) and (3) are represented in figures 4 and 5 by continuous and dotted curves, respectively, and the corresponding values of the fitting parameters A, T_c^τ, B and C in the former case, and a, T_c^τ, b and c in the latter, are listed in table 1. From the fits shown in figures 4 and 5 as well as from the reduced chi square, χ^2_r, values displayed in table 1, it is clear that both τ_1 and τ_2 exhibit logarithmic divergence at $T_c^{\tau_1} = 59.5(1)$ K and $T_c^{\tau_2} = 58.4(1)$ K, respectively, with the exponent B possessing an order of magnitude higher value in the case of τ_2.

The droplet fluctuation model [18] yields the temporal spin-autocorrelation function, $C_i(t) \equiv \langle S_i(0)S_i(t)\rangle - \langle S_i\rangle^2$, at long times, for a pure (ordered) d-dimensional Ising ferromagnet as

$$C_i(t) \sim \exp[-(t/\tau)^{(d-1)/2}] \tag{4}$$

(where τ is a correlation time that diverges as $T \to T_c$), and for a d-dimensional Ising ferromagnet with weak quenched random-exchange disorder as

$$C_i(t) \sim t^{-x(T)}. \tag{5}$$

In the case of a $d = 3$ Ising system, quenched random-exchange disorder is a relevant perturbation in the renormalization group (RG) sense and if the regions with antiferromagnetic or zero coupling exist, this model predicts that the temperature-dependent exponent x should approach zero (a finite universal value) as $T \to 0$ ($T \to T_c$). Even though Ni_3Al is not an Ising ferromagnet as it, like crystalline Ni, exhibits cubic (rather than uniaxial) magnetocrystalline anisotropy [21], a qualitative agreement between the present results and the above theoretical predictions concerning the forms of $C_i(t)$ (which is proportional

to $M_r(t)$), i.e., eqs (4) and (5), for $d = 3$ as well as the temperature dependences of the correlation time τ and exponent x becomes apparent when due consideration is given to the following. The system in question is nothing but a $d = 3$ ferromagnet with weak quenched random-exchange disorder (brought about by the residual site disorder). In such a system, quenched random-exchange disorder acts as a relevant scaling field and hence affects a cross-over in the equilibrium dynamics from the one, characteristic of a $d = 3$ pure (ordered) ferromagnet and prevalent at temperatures away from T_c, to that typical of a $d = 3$ random-exchange ferromagnet as $T \to T_c$. It is, therefore, not surprising that the exponential decay, eq. (4), and power law decay, eq. (5), completely account for the time dependence of the remanent magnetization outside and within the critical region, respectively. In the Ni_3Al sample in question, we have recently observed [20] a cross-over in the static (thermal) critical behavior from the Gaussian regime to the fixed point (characterized by the multiplicative logarithmic corrections to the mean-field power laws) as the temperature, on both sides of T_c, approaches the critical point T_c. Considering that the droplet fluctuations have more dramatic effect on dynamics than on thermodynamic (static) properties, this cross-over can be viewed as a cross-over from the static critical behavior of the pure system to the random-exchange fixed point that describes the critical behavior of a $d = 3$ ferromagnet with weak site disorder (random-exchange disorder).

The attention is next focussed on the time-evolution of the zero-field-cooled magnetization, $M_{ZFC}(t)$, starting from the time $t = 0$ when a static field of given strength is applied. Figure 9 displays the representative $M_{ZFC}(t)$ data (symbols), taken at various fixed temperatures in a field of $H = 100$ Oe without any wait time (i.e., $t_w = 0$), and the best least-squares fits (continuous curves) based on the expression

$$M_{ZFC}(t) = M_0' \left[1 - \left\{ M_1' \exp(-t/\tau_1') + (t/\tau_2')^{-\alpha'} \right\} \right] \tag{6}$$

which has a form consistent with eq. (1). A representative plot of M_{ZFC} vs. time for different wait times ($t_w = 0$ and 7200 s) at $T \cong 22$ K and $H = 100$ Oe, shown in figure 10, serves to demonstrate that no aging effects are discernible at any temperature in such experiments; the small disparity between the relaxation curves particularly at short times ($t < 50$ s) is traceable to the slight difference in temperature. A perfect agreement between the data and the fits noticed in figure 9 bears a testimony to the fact that eq. (6) forms an excellent description of the observed time dependence of M_{ZFC} at all temperatures except for $T = 72.189$ K; at this temperature ($T \gg T_c$), instead of eq. (6), the expression $M_{ZFC}(t) = M_0'[M_1' \exp(-t/\tau_1') + (t/\tau_2')^{-\alpha'}]$ fits the $M_r(t)$ data better. Figure 9 shows the best theoretical fit (continuous curve), based on the latter expression, for the $M_{ZFC}(t)$ data taken at this temperature. The optimum values of the free fitting parameters $M_0', M_1', \tau_1', \tau_2'$ and α' obtained at different temperatures are plotted against temperature in figures 11–13. Note that the $M_{ZFC}(t)$ data taken at $T > T_c$ in $H = 10$ Oe and $H = 100$ Oe have been corrected for the diamagnetic contribution arising from the empty sample holder. Such corrections, determined from the empty sample holder runs at $H = 10$ Oe and 100 Oe, become necessary at such temperatures.

The striking features presented by the temperature variations of the parameters are the following: (I) $M_0'(T)$ at $H = 10$ Oe exhibits the demagnetization-limited-like behavior, typical of ferromagnets, at temperatures below the zero-field Curie temperature [20] $T_c(0) = 56.377$ K. (II) For $T \leq 0.9T_c(H)$ (field-dependent T_c, to be defined later), M_0' and M_1' depend sensitively on field and, to a lesser extent, on temperature, τ_1' and α' are insensitive to both field and temperature whereas τ_2' is temperature-independent but depends

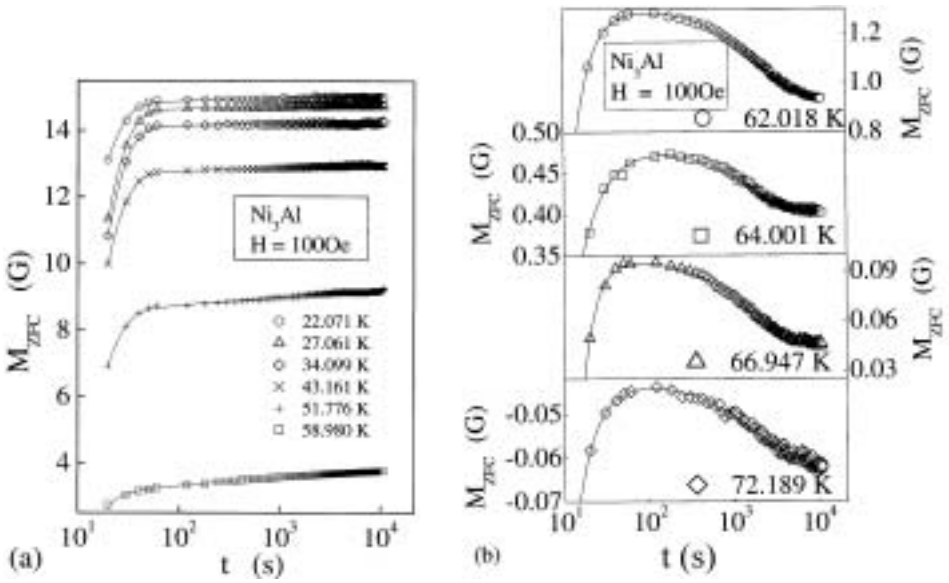

Figure 9. The $M_{\rm ZFC}(t)$ data (symbols) taken at different temperatures and $H = 100$ Oe and the corresponding best least-squares fits (solid curves) based on eq. (6).

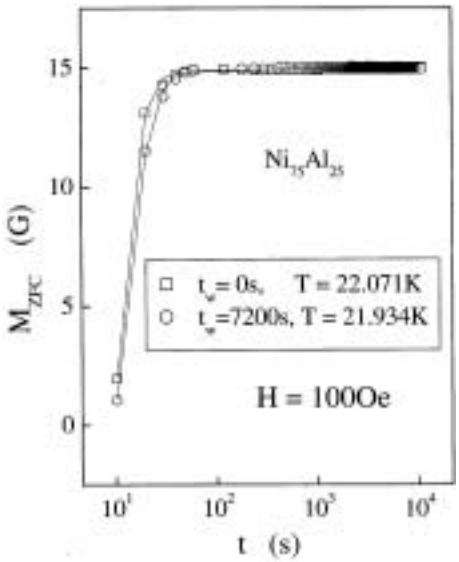

Figure 10. Representative $M_{\rm ZFC}(t)$ data taken at $H = 100$ Oe and widely different wait time, $t_{\rm w}$, values, showing the absence of aging effects (see text).

on field such that $\tau_2'(H = 10\ \text{Oe}) > \tau_2'(H = 100\ \text{Oe})$. (III) At $T > 0.9T_{\rm c}(H)$, M_0' and M_1' drop rapidly and change sign at $T_0 \cong T_{\rm c}(H)$, α' increases steeply to reach a peak at $T \cong T_{\rm c}(H)$, while τ_1' and τ_2' exhibit a singular behavior. As in the case of $M_{\rm r}(t)$ data, the

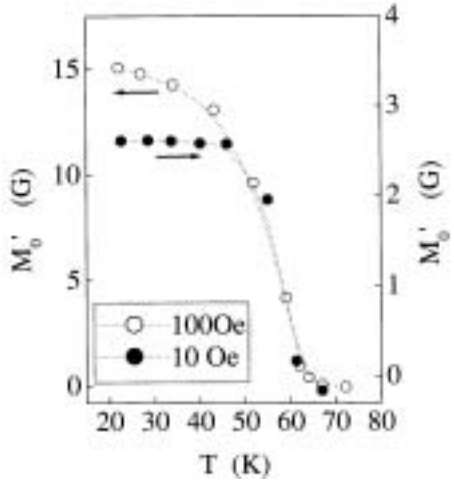

Figure 11. Magnetization M_0' vs. temperature in the presence of field $H = 10$ Oe (solid circles) and 100 Oe (open circles). Horizontal arrows indicate the relevant ordinate scales.

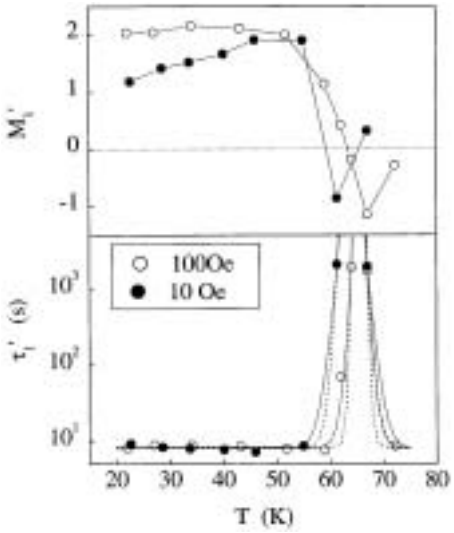

Figure 12. Prefactor, M_1', and relaxation time, τ_1', as functions of temperature for fields $H = 10$ Oe (solid circles) and 100 Oe (open circles). The continuous (dotted) curve in the lower panel represents the logarithmic fit (power law fit).

observations (II) and (III) basically reflect the fact that power law and exponential relaxation mainly govern the behavior of $M_{\rm ZFC}(t)$ within and outside the critical region, respectively. The singular behavior of the relaxation times τ_1' and τ_2', like those of τ_1 and τ_2, has been analysed using expressions (2) and (3) with the result that logarithmic divergence again provides a better description (more convincingly for τ_2') of the observed critical behavior of τ_1' and τ_2' than a simple power law does. That this is indeed the case is made clear by the optimum fits based on eqs (2) and (3), shown in figures 12 and 13 as continuous and dotted curves, respectively, and by the values of $\chi_{\rm r}^2$ displayed in table 2. This table also lists the optimum values of the parameters A', $T_{\rm c}^{\tau'}(H), B'$ and C' ($a', T_{\rm c}^{\tau'}(H), b'$ and c') for the fit based on eq. (2) (eq. (3)). $T_{\rm c}^{\tau'}(H)$ represents the temperature at which τ_1' or τ_2' diverges for a given value of H. From the entries in table 2, it is evident that for a given value of H, $\tau_1'(T)$ and $\tau_2'(T)$ data yield the same value for the critical temperature within the uncertainty limits, $T_{\rm c}^{\tau'}(H)$ assumes a higher value with increasing field strength and that the logarithmic exponent B' is field-independent (within the error bars). At this stage it should be emphasized that even though essentially five $\tau(T)$ data points in the critical region are able to clearly distinguish between the logarithmic and power law divergences in the present case, a much larger number of data points in the critical region are needed to refine the value of the critical temperature, $T_{\rm c}^{\tau}$, and hence, that of the critical exponent, B, which characterizes the logarithmic divergence in $\tau(T)$ at $T = T_{\rm c}^{\tau}$.

Even though the droplet fluctuation model [18] does not consider the 'in-field' relaxation of zero-field-cooled magnetization per se, some of the above observations do find a qualitative interpretation in terms of this model. In this model, the effect of external magnetic field

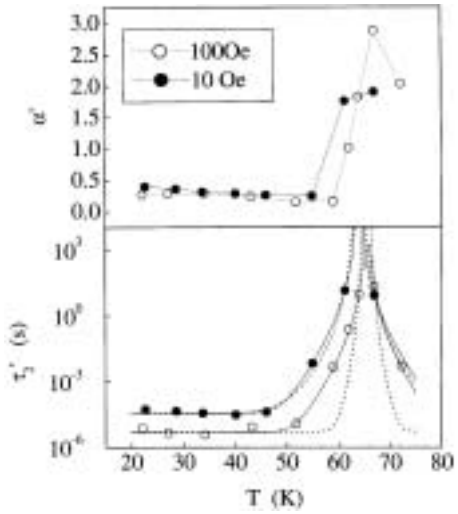

Figure 13. Exponent, α', and relaxation time, τ_2', as functions of temperature for fields $H = 10$ Oe (solid circles) and 100 Oe (open circles). The continuous (dotted) curve in the lower panel represents the logarithmic fit (power law fit).

is to suppress the droplet fluctuations and hence, in moderate or low fields, the long-time behavior of the temporal spin-autocorrelation function, i.e., eqs (4) and (5), remains unaltered but the temperature at which τ_1' diverges is expected to increase with field, consistent with the present observation. A droplet, whose free energy is considerably less than the average, is formed when the domain wall surrounding the droplet passes through regions of weak ferromagnetic coupling, brought into existence by quenched site (or equivalently, random-exchange) disorder, and thus the local domain-wall free energy is reduced. Such a droplet is long-lived because the domain wall is pinned to the regions of weak ferromagnetic coupling (e.g., the regions surrounding the finite ferromagnetic clusters in the $d = 3$ infinite ferromagnetic network plus finite ferromagnetic cluster models proposed earlier by Coles *et al* [22] and Kaul [23]) and in order to dissolve the droplet, the domain wall must move away from these favorable locations and cross a large free-energy barrier. Higher the external magnetic field strength, easier it is for the domain wall to cross the barrier (or, in other words, to get depinned) and hence shorter the lifetime of the droplet. It immediately follows that τ_2' should decrease with increasing field, as is indeed observed.

The existing theories, including the droplet fluctuation model, fail to provide any explanation for the present findings such as: (a) logarithmic divergence of τ_1 (τ_1') and τ_2 (τ_2'), (b) insensitivity of τ_1' and α' to both field and temperature for $T \leq 0.9T_c(H)$, (c) practically no dependence on temperature of τ_2' (τ_2 and α) for a given field strength (at zero field) and $T \leq 0.9T_c(H)$ ($\leq 0.9T_c(0)$), and (d) the observation (III) above.

4. Summary and conclusion

With a view to study magnetic relaxation in a ferromagnet with weak quenched random-exchange disorder, two types of time-dependent measurements, namely, the isothermal

Table 2. Optimum values for the fit parameters appearing in eqs (2) and (3).

(a) for $H = 10$ Oe

	A' (s)	$T_c^{\tau'}$ (K)	B'	C' (s)	χ_r^2 (10^{-3})	a' (s)	$T_c^{\tau'}$ (K)	b'	c' (s) (10^{-5})	χ_r^2 (10^{-3})
τ_1'										
Logarithmic divergence, eq. (2)	1.2(1) $\times 10^{-5}$	64.1(1)	16.6(1)	7.9(1)	4.1	1.2(1) $\times 10^{-5}$	64.1(1)	16.6(1)	7.9(1)	4.1
Power law divergence, eq. (3)	9.5(1) $\times 10^{-12}$	64.1(2)	−8.4(1)	8.0(1)	4.5	9.5(1) $\times 10^{-12}$	64.1(2)	−8.4(1)	8.0(1)	4.5
τ_2'										
Logarithmic divergence, eq. (2)	1.6(1) $\times 10^{-7}$	64.0(1)	15.9(1)	3.8(1)	2.2	1.6(1) $\times 10^{-7}$	64.0(1)	15.9(1)	3.8(1)	2.2
Power law divergence, eq. (3)	2.3(1) $\times 10^{-16}$	64.0(2)	−7.1(1)	3.4(1)	8.9	2.3(1) $\times 10^{-16}$	64.0(2)	−7.1(1)	3.4(1)	8.9

(b) for $H = 100$ Oe

τ_1'										
Logarithmic divergence, eq. (2)	9.6(1) $\times 10^{-7}$	65.5(1)	16.0(1)	8.1(1)	0.2	9.6(1) $\times 10^{-7}$	65.5(1)	16.0(1)	8.1(1)	0.2
Power law divergence, eq. (3)	3.2(1) $\times 10^{-12}$	65.5(2)	−8.9(1)	8.2(1)	2.0	3.2(1) $\times 10^{-12}$	65.5(2)	−8.9(1)	8.2(1)	2.0
τ_2'										
Logarithmic divergence, eq. (2)	7.3(1) $\times 10^{-9}$	65.6(1)	16.0(1)	4.8(1)	0.47	7.3(1) $\times 10^{-9}$	65.6(1)	16.0(1)	4.8(1)	0.47
Power law divergence, eq. (3)	2.3(1) $\times 10^{-16}$	65.5(1)	−10(1)	5.2(1)	3.8	2.3(1) $\times 10^{-16}$	65.5(1)	−10(1)	5.2(1)	3.8

remanent magnetization decay, $M_r(t)$, and the 'in-field' growth of zero-field-cooled magnetization, $M_{ZFC}(t)$, with time, have been performed on a nearly ordered (long-range atomic order parameter $= 0.95 \pm 0.02$) sample of the weak itinerant-electron ferromagnet, Ni_3Al, in the temperature range $0.25T_c \leq T \leq 1.25T_c$, where T_c is the Curie temperature. None of the expressions proposed hitherto for describing $M_r(t)$ in quenched random spin systems in the literature, but only the following expressions for $M_r(t)$ and $M_{ZFC}(t)$

$$M_r(t) = M_0[M_1 \exp(-t/\tau_1) + (t/\tau_2)^{-\alpha}]$$

and

$$M_{\rm ZFC}(t) = M_0' \left[1 - \{M_1' \exp(-t/\tau_1') + (t/\tau_2')^{-\alpha'}\}\right]$$

are found to reproduce such data very closely. An elaborate analysis of the data based on these expressions reveals several interesting aspects of magnetic relaxation in the ferromagnetic system in question that include the following: (i) No aging effects have been observed in $M_{\rm r}(t)$ or $M_{\rm ZFC}(t)$ at any temperature. (ii) The power law decay (growth) and the exponential decay (growth) essentially determine the time dependence of remanent magnetization, $M_{\rm r}(t)$ (zero-field-cooled magnetization $M_{\rm ZFC}(t)$, in the presence of external magnetic field, H) within and outside the critical region, respectively. (iii) The relaxation times $\tau_1(T)(\tau_1'(T))$ and $\tau_2(T)(\tau_2'(T))$ exhibit logarithmic divergence at critical temperatures $T_{\rm c}^{\tau_1}(T_{\rm c}^{\tau_1'}(H))$ and $T_{\rm c}^{\tau_2}(T_{\rm c}^{\tau_2'}(H))$. (iv) $T_{\rm c}^{\tau_1'}(H)$ and $T_{\rm c}^{\tau_2'}(H)$ increase with H such that at any given field value, $T_{\rm c}^{\tau_1'} = T_{\rm c}^{\tau_2'}$. (v) The exponent $B(B')$, characterizing the logarithmic divergence of $\tau_1(T), \tau_2(T)(\tau_1'(T), \tau_2'(T))$, possesses an order of magnitude higher value for τ_2 compared to that for τ_1 (field-independent value of $B' \simeq 16$ for both τ_1' and τ_2'). (vi) For $T \leq 0.9T_{\rm c}^{\tau}$ ($T \leq 0.9T_{\rm c}^{\tau'}(H)$), τ_1, τ_2 and α are temperature-independent (τ_1' and α' are insensitive to both field and temperature whereas τ_2' is temperature-independent but depends on field such that $\tau_2'(H = 10\ \text{Oe}) > \tau_2'(H = 100\ \text{Oe})$), where $T_{\rm c}^{\tau}(T_{\rm c}^{\tau'}(H))$ stands for both $T_{\rm c}^{\tau_1}$ and $T_{\rm c}^{\tau_2}$ $(T_{\rm c}^{\tau_1'}(H))$ and $(T_{\rm c}^{\tau_2'}(H))$; in the same temperature range, i.e., for $T \leq 0.9T_{\rm c}^{\tau}$ or $0.9T_{\rm c}^{\tau'}(H)$, α and α' have widely different (by orders of magnitude) values but $\tau_1 = \tau_1' \simeq 9.8$ s. Within the framework of the droplet fluctuation model, the above observation (ii) is a manifestation of a cross-over in the equilibrium dynamics from the one characteristic of a pure $d = 3$ ferromagnet (in which atomic ordering is complete) and prevalent at temperatures away from $T_{\rm c}$, to that typical of a $d = 3$ random-exchange ferromagnet, as $T \to T_{\rm c}$, caused by quenched random-exchange disorder, which is a *relevant* perturbation in the renormalization group sense in the present case. Barring certain aspects of magnetic relaxation that find, at best, a *qualitative* explanation in terms of the droplet fluctuation model, most of the above findings expose the inadequacy of the existing theories in that they fail to offer any explanation for most of the observations listed above.

Acknowledgements

This work was supported by the Department of Science and Technology, India, under the Grant No. SP/S2/M-21/97. AS gratefully acknowledges the financial support received from the Council of Scientific and Industrial Research, India.

References

[1] L Lundgren, P Svedlindh, P Nordblad and O Beckman, *Phys. Rev. Lett.* **51**, 911 (1983)

[2] R V Chamberlin, G Mozurkewich and R Orbach, *Phys. Rev. Lett.* **52**, 867 (1984); *Phys. Rev.* **B52**, 867 (1984)

[3] M Alba, M Ocio and J Hammann, *J. de Phys. Lett. (Paris)* **46**, L1101 (1985); *Europhys. Lett.* **2**, 45 (1986)
R Hoogerbeets, W-L Luo and R Orbach, *Phys. Rev.* **B34**, 1719 (1986)
L Lundgren, P Nordblad and P Svedlindh, *Phys. Rev.*, **B34**, 8164 (1986)

[4] K Gunnarsson, P Svedlindh, P Nordblad and L Lundgren, *Phys. Rev. Lett.* **61**, 754 (1988)

[5] P Granberg, L Sandlund, P Nordblad, P Svedlindh and L Lundgren, *Phys. Rev.* **B38**, 7097 (1988)
[6] P Granberg, L Lundgren and P Nordblad, *J Magn. Magn. Mater.* **92**, 228 (1990)
[7] M Lederman, R Orbach, J M Hammann, M Ocio and E Vincent, *Phys. Rev.* **B44**, 7403 (1991)
F Lefloch, J Hammann, M Ocio and E Vincent, *Europhys. Lett.* **18**, 647 (1992) and references cited therein
[8] P D Mitchler, R M Roshko and W Ruan, *Philos. Mag.* **B68**, 539 (1993)
H Rieger, *J. Phys.* **A26**, L615 (1993)
[9] G C DeFotis and K D Dell, *Phys. Rev.* **B50**, 9937 (1994)
[10] C Djurberg, P Granberg, J Mattsson and P Nordblad, *Phys. Rev.* **B50**, 15775 (1994)
[11] D S Fisher and D A Huse, *Phys. Rev.* **B38**, 373 (1988)
[12] G J M Koper and H J Hilhorst, *J. de Phys. (Paris)* **49**, 429 (1988)
[13] M Nifle and H J Hilhorst, *Phys. Rev. Lett.* **67**, 2992 (1992)
[14] J O Andersson, J Mattsson and P Svedlindh, *Physica* **B194–196**, 307 (1994); *Phys. Rev.* **B49**, 1120 (1994)
[15] P Mitchler, R M Roshko and W Ruan, *J. Appl. Phys.* **73**, 5460 (1993)
[16] D Li, R M Roshko and G Yang, *J. Appl. Phys.* **75**, 5844 (1994); *Phys. Rev.* **B49**, 9601 (1994)
[17] K Jonason, J Mattsson and P Nordblad, *Phys. Rev. Lett.* **77**, 2562 (1996)
[18] D A Huse and D S Fisher, *Phys. Rev.* **B35**, 6841 (1987)
[19] R V Chamberlin and D N Haines, *Phys. Rev. Lett.* **65**, 2197 (1990)
[20] A Semwal and S N Kaul, *Phys. Rev.* **B64**, 014417 (2001); *J. Phys.: Condens. Matter* **14**, 5829 (2002)
[21] T I Sigfusson and G G Lonzarich, *Phys. Scr.* **25**, 720 (1982)
[22] B R Coles, B V B Sarkissian and R H Taylor, *Philos. Mag.* **B37**, 489 (1978)
[23] S N Kaul, *Solid State Commun.* **36**, 279 (1980); *IEEE Trans. Magn.* **MAG-20**, 1290 (1984); *J. Magn. Magn. Mater.* **53**, 5 (1985); *J. Phys.: Condens. Matter* **3**, 4027 (1991)